CLASSICAL vs MODERN MAGNETIC ATTITUDE CONTROL DESIGN: A CASE STUDY

Tiziano Pulecchi[1], Marco Lovera[1], Andras Varga[2]
[1]*Dipartimento di Elettronica e Informazione, Politecnico di Milano*
P.za Leonardo da Vinci 32, 20133 Milano, Italy
[2]*German Aerospace Center, DLR-Oberpfaffenhofen*
Institute of Robotics and Mechatronics, D-82234 Wessling, Germany
lovera@elet.polimi.it

INTRODUCTION

Electromagnetic actuators are a particularly effective and reliable technology for attitude control of small satellites. As is well known, the main difficulty in the design of attitude control laws based on such actuators is related to the fact that magnetic torques are instantaneously constrained to lie in the plane orthogonal to the local direction of the geomagnetic field vector. Controllability of attitude dynamics is ensured for a wide range of orbit altitudes and inclinations in spite of this constraint, thanks to the variability of the geomagnetic field. However, this implies that the attitude control engineer has to deal with a time-varying model in the control design process. A considerable effort has been devoted to the analysis of this control problem; in particular, as far as the linear attitude regulation problem is concerned, two main lines of work can be identified in the literature.

Classical methods are based on the use of averaged models, i.e., on the idea of replacing the actual time-varying dynamics of the magnetically actuated spacecraft with an approximate time-invariant model obtained using averaging techniques. Clearly, the advantage of this approach is that the control problem becomes time-invariant, however the designer is left with the burden of verifying *a posteriori* that the designed controller actually stabilises the original time-varying dynamics and achieves a satisfactory performance level. This averaging approach, originally proposed in [1], was further developed in [2] to deal with the stabilisation problem for the coupled roll/yaw dynamics of a momentum biased spacecraft using a magnetic torquer aligned with the pitch axis.

More recently, design methods based on full periodic models have been proposed. As the variability of the geomagnetic field is almost time-periodic, most of the recent work on the linear magnetic attitude control problem has focused on the use of optimal and robust periodic control theory for the design of state and output feedback regulators. While periodic control design methods have the significant advantage of guaranteeing closed loop stability *a priori*, they unfortunately lead to the synthesis of time-periodic regulators, which would be extremely impractical to implement and operate. Therefore, the main current research efforts in this area aim at developing sound design methods leading to constant gain controllers (see, e.g., [3, 4] and the recent survey paper [5]) while ensuring closed loop stability and some specified level of performance.

In the light of the above discussion, the aim of the paper is compare the results obtained in the design of magnetic attitude control systems using classical (i.e., based on averaging) and modern (i.e., based on periodic models) methods for the tuning of the control algorithms. Specific reference will be made to the case of roll/yaw stabilization for a momentum bias LEO spacecraft. More precisely, classical methods such as the ones reported in [2] are compared with the approach of [4] to the design of digital attitude controllers for spacecraft equipped with magnetic actuators. This approach allows the design of periodic control laws (of the so-called ”projection based” class, an architecture widely used in the practice of magnetic attitude control) parameterised via constant gains with guaranteed nominal stability and LQ performance, using an optimisation-based method.

ROLL/YAW DYNAMICS OF A MOMENTUM BIAS SPACECRAFT

In this paper we focus on the synthesis of a unique pitch dipole, magnetic attitude controller supervising roll/yaw control for an Earth-pointing momentum bias satellite in a circular orbit. The satellite momentum wheel is aligned along the spacecraft's pitch axis (*i.e.*, opposite to the orbital normal) and rotating counterclockwise.

As is well known (*e.g.*, see [6]), this configuration is stable as far as roll/yaw dynamics is concerned, so the attitude controller only needs to compensate for the satellite precession and nutation induced by external disturbance torques. This goal can be conveniently achieved using a single magnetic coil aligned to the spacecraft's pitch axis, provided of course that the orbit's inclination is not too small.

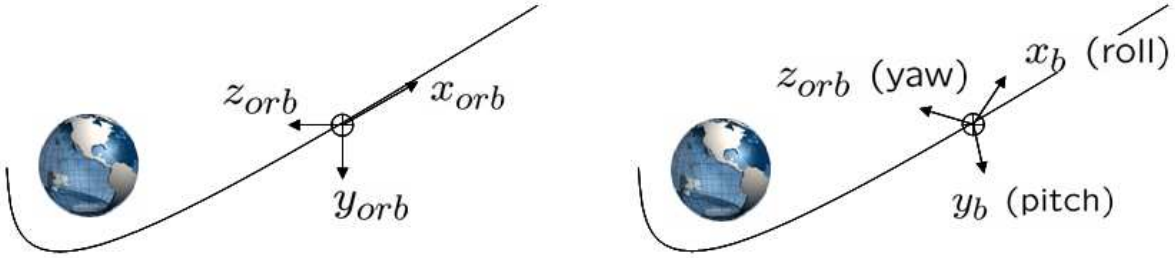

(a) Orbital frame of reference.

(b) Spacecraft body axes.

Fig. 1. Comparison between the spacecraft (roll, pitch, yaw) body axes and orbital reference system.

Coupled roll/yaw dynamics

The adoption of a momentum bias configuration typically grants very high control performance. Hence, the description of the satellite angular dynamics by simplified linearized mathematical models, holding under the approximation of "infinitesimal" angles, is justified. These models only are amenable to the analysis proposed in [2]. It must be stressed that their adoption in lieu of the complete Euler equations is required only by the pole placement reference design approach. However, since the goal here is to compare the benefits of innovative design techniques with respect to the classical pole placement one, the simplified model will be input to all of the considered design procedures, in order to avoid the introduction of a possibly severe seed of performance mismatch from the very outset.

The Euler equations describing the angular dynamics of a satellite equipped with a momentum wheel of given constant angular momentum h_w read

$$\dot{h} + \omega \times (h + h_w) = T \ , \tag{1}$$

where h is the satellite angular momentum, ω is its angular rate in the rotating frame, and T is the applied torque.

Consider now the local vertical, local horizontal orbital frame, depicted in Fig. 1(a), with the y axis opposite to the orbit normal, x and z axes directed along the velocity vector and nadir, respectively. Also, assume that the roll, pitch and yaw axes (see Fig. 1(b)) are principal axes and the angles α_1, α_2, α_3 to rotate the body frame into the orbital frame are very small[1]. Denote by ω_0 the angular velocity of the orbital frame, by $\omega = [\omega_1 \ \ -\omega_0 + \omega_2 \ \ \omega_3]^T$ the spacecraft's angular velocity and by $I_1, \ I_2, \ I_3$ its moments of inertia along the roll, pitch and yaw axes respectively. Then, the nominal angular rate of the satellite as seen in the orbital frame is $\Omega_0 = [0 \ \ -\omega_0 \ 0]^T$, whereas the momentum wheel has angular momentum vector $h_w = [0 \ \ h_s \ \ 0]^T$, with $-\omega_0, h_s < 0$.

Assume further that $|h_w| \ \gg \ \max(I_1, I_3)\,|\omega_0|$, which of course is the case for a momentum bias Earth pointing satellite. Then, the linearized Euler equations for the roll/yaw axes of a momentum bias satellite specialize into

$$\begin{aligned} I_1\ddot{\alpha}_1 - h_s\dot{\alpha}_3 - \omega_0\, h_s\alpha_1 &= T_1 \\ I_3\ddot{\alpha}_3 + h_s\dot{\alpha}_1 - \omega_0\, h_s\alpha_3 &= T_3 \ . \end{aligned} \tag{2}$$

Since the only torque producing device onboard is the pitch magnetic coil of dipole m_2, the (magnetic) control torque arising from the interaction with the planet's magnetic field b is in the form

$$T_m^T = [T_1 \ \ T_3] = [b_3 \ \ -b_1]\, m_2 \ . \tag{3}$$

We therefore get to the following compact matrix description of the roll/yaw angular dynamics

$$\dot{x} = A\,x + Bu \tag{4}$$

where $x^T = [\alpha_1, \ \alpha_3, \dot{\alpha}_1, \ \dot{\alpha}_3]$, $u^T = [\, b_3 \quad -b_1\,]\, m_2$ and

$$A = \begin{bmatrix} 0 & 0 & 1 & 0 \\ 0 & 0 & 0 & 1 \\ \frac{\omega_0\, h_s}{I_1} & 0 & 0 & \frac{h_s}{I_1} \\ 0 & \frac{\omega_0\, h_s}{I_3} & -\frac{h_s}{I_3} & 0 \end{bmatrix}, \ B = \begin{bmatrix} 0 & 0 \\ 0 & 0 \\ \frac{1}{I_1} & 0 \\ 0 & \frac{1}{I_3} \end{bmatrix}. \tag{5}$$

[1]The two assumptions imply that the satellite's inertia matrix is diagonal and its angular rate vector $\omega = [\omega_1 \ \omega_2 \ \omega_3]^T \simeq [\dot{\alpha}_1 \ \dot{\alpha}_2 \ \dot{\alpha}_3]^T$

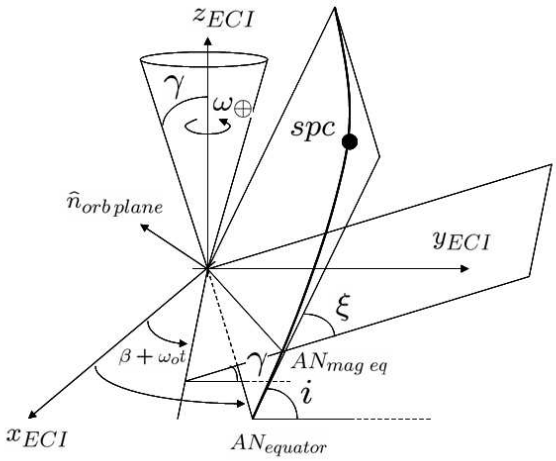

Fig. 2. The geomagnetic field tilted dipole model.

The Geomagnetic Field Tilted Dipole Model

The geomagnetic field tilted dipole model, depicted in Fig. 2, will be used in the following for control design purposes. According to the tilted dipole model, the magnetic field sensed by an Earth-pointing satellite orbiting on a circular orbit, perfectly aligned with the rotating orbital frame is given by

$$b = \frac{\mu_m}{r^3} \begin{bmatrix} \sin\xi\ \cos\theta \\ -\cos\xi \\ 2\ \sin\xi\ \sin\theta \end{bmatrix} \tag{6}$$

where

$$\begin{aligned} \theta &= \omega_0 t - \eta \\ \cos\xi &= \cos i\ \cos\gamma + \sin i\ \sin\gamma\ \cos\beta' \\ \sin\eta\ \sin\xi &= -\sin\gamma \\ \cos\eta\ \sin\xi &= \sin i\ \cos\gamma - \cos i\ \sin\gamma\ \cos\beta' \\ \beta' &= \beta_0 + \omega_\oplus t - \Omega_{an}. \end{aligned}$$

With reference to Fig. 2, $\gamma = 11.44^\circ$ is the dipole tilt; $\mu_m = 7.943 \times 10^{15}\, Wbm$ is the Earth's magnetic dipole strength; r is the orbital radius; ξ is the instantaneous inclination of the orbital plane *w.r.t.* the geomagnetic equator; η is the angle between the ascending nodes of the orbit relative to the Earth's equator and the geomagnetic equator; Ω_{an} is the orbit's ascending node angle; i the orbit inclination; $\omega_0 t$ the satellite true anomaly; and finally $\beta_0 + \omega_\oplus t$ is the angle formed between the vernal equinox and the intersection of the orbit with the geomagnetic equator. ($\omega_\oplus$ denotes, as usual, the Earth's rotation rate.) Subsequent to the Earth's spinning, ξ oscillates between $i - \gamma$ and $i + \gamma$, whereas η ranges within the interval $-\gamma$, γ in a day.

ROLL-YAW STABILISATION OF MOMENTUM BIAS SATELLITES: CLASSICAL vs MODERN CONTROL

Two different approaches for the synthesis of the pitch dipole control law will be considered in this paper and their performance compared: the "classic" pole placement design proposed in [2] and the projection-based, numerically optimized output feedback technique discussed in [4]. The former approach, which relies on a "smart" averaging of the system's periodic components, adopts a "minimal" three gains control scheme aiming to control precession, damp nutations and stiffen the roll/yaw motion directly. The latter, on the other hand, leads to a tuning method for a full gain matrix as it relies on a full periodic model for the coupled roll/yaw dynamics.

Recalling (3), in the pole placement approach the magnetic control law is expressed in the form

$$m_2 = [b_3 \quad -b_1](K\, y)\ , \tag{7}$$

where K is the controller gain matrix and y is some set of available attitude-relevant measures. The magnetic torques on the roll and yaw axes are then given by

$$T_m = \begin{bmatrix} b_3^2 & -b_1 b_3 \\ -b_1 b_3 & b_1^2 \end{bmatrix} K\, y. \tag{8}$$

If (8) is now averaged over the orbital period, under the approximation $\omega_0 \gg \omega_\oplus$ we get

$$T_{m\,ave} = \hat{\mu}_m^2 \sin^2 \xi \begin{bmatrix} 2 & 0 \\ 0 & 0.5 \end{bmatrix} K\, y, \tag{9}$$

where $\hat{\mu}_m^2 = \left(\frac{\mu_m}{r^3}\right)^2$, which is a generalization of the formulas presented in [2] and adopted therein, together with the dynamic model for roll/yaw dynamics given by (4)-(5) for stability analysis and pole placement based controller synthesis. The control design problem is therefore recast, subject to the approximations due to averaging, as an LTI one.

We will hereafter compare the pole placement-based technique presented in [2] with the fixed-structure, projection based output feedback control laws introduced in [4], in the form

$$m_2 = \frac{1}{b_1^2 + b_3^2}[b_3 \;\; -b_1](K\, y), \tag{10}$$

where the control gain is numerically optimized in order to achieve simultaneously several design specifications. To this end, note that recalling again (3) the roll/yaw magnetic torques resulting from adoption of (10) are in the form

$$T_m = \Gamma(t) K\, y = \frac{1}{b_1^2 + b_3^2} \begin{bmatrix} b_3^2 & -b_1 b_3 \\ -b_1 b_3 & b_1^2 \end{bmatrix} K\, y\,, \tag{11}$$

where, exploiting (6), an explicit time-periodic expression for matrix $\Gamma(t)$ can be obtained, as

$$\Gamma(t) = \frac{\sin^2(\xi)}{1 + 3\sin^2(\xi)\sin^2(\theta)} \begin{bmatrix} 4\sin^2(\theta) & -\sin(2\theta) \\ -\sin(2\theta) & \cos^2(\theta) \end{bmatrix}. \tag{12}$$

If we recall that the orbit periodicity is much shorter than the Earth's rotation period, by substituting ξ and η with their average values, the terms in (12) can be rearranged in the more convenient form

$$\Gamma(t) = \frac{\sin^2(i)}{1-z} \begin{bmatrix} 2 & 0 \\ 0 & .5 \end{bmatrix} + \frac{\sin^2(i)}{1 - z + z\,\cos(2\omega_0 t)} \begin{bmatrix} -\frac{2\,\cos(2\omega_0 t)}{(1-z)} & -\sin(2\omega_0 t) \\ -\sin(2\omega_0 t) & \frac{(1-2z)\,\cos(2\omega_0 t)}{2(1-z)} \end{bmatrix}, \tag{13}$$

where we adopted the notation $z = -\frac{3}{2}\,\sin^2(i)$. Equations (11) and (13), together with the dynamic model for roll/yaw dynamics given by (4)-(5) represent the design model used in the periodic output feedback control design approach. As is apparent from the above discussion, in this case we are dealing with an LTP system and no approximations in the derivation of the design model have been introduced.

POLE PLACEMENT DESIGN

In [2] a magnetic controller for a momentum bias spacecraft equipped with a single pitch electromagnet was proposed. The controller , augmenting the magnetic angular momentum removal feedback in order to incorporate a stiffness gain k_s, besides the precession and nutation gains k_p and k_n, was defined as follows:

$$m_2 = k_p\, h_w\, (b_1\alpha_1 + \chi_p b_3 \alpha_3) - k_n\, (b_3 \dot{\alpha}_1 - \chi_n b_1 \dot{\alpha}_3) - k_s\, (b_3 \alpha_1 - \chi_s b_1 \alpha_3)\,, \tag{14}$$

where k_p, k_n, k_s, χ_p, χ_n and χ_s are the design parameters. Note that the form of the last term, the stiffness term, resembles that of the nutation damping term because they are both intended to influence the roll and yaw angles and rates directly.

If (14) is adopted, the average magnetic control torques can be written in the form

$$\begin{aligned} T_{m1\,ave} &= -2k_n' \dot{\alpha}_1 + 2k_p' h_s \chi_p \alpha_3 - 2k_s' \alpha_1 \\ T_{m3\,ave} &= -\frac{1}{2} k_n' \chi_n \dot{\alpha}_3 - \frac{1}{2} k_p' h_s \alpha_1 - \frac{1}{2} k_s' \chi_s \alpha_3, \end{aligned} \tag{15}$$

where $k'_p = (\hat{\mu}_m^2\, sin^2\xi_m)\, k_p$, $k'_n = (\hat{\mu}_m^2\, sin^2\xi_m)\, k_n$ and $k'_s = (\hat{\mu}_m^2\, sin^2\xi_m)\, k_s$.

Now, if we substitute (15) in the simplified roll/yaw angular dynamics equations of a momentum bias, Earth-pointing spacecraft in a circular orbit (2), and adopt the notation $\hat{k}_{n1} = k'_n/(I_1\omega_0)$, $\hat{k}_p = k'_p/\omega_0$, $\hat{k}_{s1} = k'_s/(I_1\omega_0^2)$, $i_a = I_1/I_3$ (roll/yaw inertia asymmetry parameter), $\hat{J}_{si} = h_s/(I_i\omega_0)$, $i \in \{1, 3\}$ (momentum bias parameters), we get for the coupled roll/yaw angular dynamics the following characteristic equation

$$s^4 + a_1 s^3 + a_2 s^2 + a_3 s + a_4 = 0,$$

with

$$\begin{aligned}
a_1 &= \hat{k}_{n1}(2 + \frac{1}{2} i_a \chi_n) \\
a_2 &= 2\hat{k}_{s1} - \hat{J}_{s1} + i_a(\hat{k}_{n1}^2 + \frac{1}{2}\hat{k}_{s1}\chi_s - \hat{J}_{s1} + \hat{J}_{s1}^2) \\
a_3 &= i_a[\frac{1}{2}\hat{k}_{n1}\chi_n(-\hat{J}_{s1} + 2\hat{k}_{s1}) + 2\hat{k}_{n1}(-\hat{J}_{s1} + \frac{1}{2}\hat{k}_{s1}\chi_s) + \hat{J}_{s1}^2\hat{k}_p(\frac{1}{2} + 2\chi_p)] \\
a_4 &= i_a[(-\hat{J}_{s1} + \frac{1}{2}\hat{k}_{s1}\,\chi_s)(-\hat{J}_{s1} + 2\hat{k}_{s1}) + \hat{J}_{s1}^2\hat{k}_p^2\,\chi_p] \,.
\end{aligned}$$

The Routh-Hurwitz stability analysis yields the following necessary and sufficient conditions for asymptotic stability:

$$a_i > 0,\ i = 1, \ldots, 4, \quad \Delta_3 = a_1(a_2\, a_3 - a_1 a_4) - a_3^2 > 0$$

Anyway, with lengthy coefficients and several parameters involved, it is infeasible to develop a simple parametric inequality. Special cases of the modulation policy (14) have therefore been considered:

- Alfriend's Law [1]. Stickler and Alfriend's modulation policy can be obtained as a specialization of (14) by setting $k_s = 0$, $\chi_n = 1$ and $\chi_p = 0$.
- Wheeler's Law [7]. Wheeler analyzed a pitch dipole modulation policy that uses yaw and yaw rate, in addition to roll and roll rate. This policy can be obtained from (14) by substituting $k_s = 0$, $\chi_n = 1$ and $\chi_p = 1$.
- Lebsock-Eterno's Law [8]. In order to symmetrize the average roll/yaw control torques the setting $h_s k'_p = -4k'_s$, $\chi_n = 4 = \chi_s$, $\chi_p = 1/4$ can be adopted, which leads exactly to the modulation policy studied by Lebsock and Eterno.

The pole placement technique relies on a distinctive property of system (2), namely the marked frequency separation between its precession and nutation motions. Indeed, the eigenanalysis of the free motion of (2) reveals the two complex conjugate pairs of eigenvalues

$$\pm j|\omega_0| \,, \qquad \pm j\frac{|h_s|}{\sqrt{I_1 I_3}}$$

characterizing the spacecraft precession and nutation. Under the assumption $|h_s| \gg \max(I_1,\, I_3)\, |\omega_0|$, a large frequency separation is observed, the nutation frequency being typically $50 - 2000$ times larger than the precession frequency ω_0 in the rotating orbital frame. Therefore, for a preliminary determination of the control gains it appears quite convenient and fairly accurate to treat precession and nutation separately.

Precession Control

The roll/yaw nutation-free dynamics of a momentum bias Earth pointing spacecraft can be described in the orbital frame by

$$\begin{cases} \dot{x_1} - \omega_0 x_3 = T_1 \\ \dot{x_3} + \omega_0 x_1 = T_3 \end{cases} \tag{16}$$

where $T_1,\, T_3$ represent the terms of the average magnetic torques (15) pertaining to the precession mode only (k_n is set to zero in (7)), obtained as a specialization of the more general (8), and $[x_1 \;\; x_3] = [-h_w\alpha_3 \;\; h_w\alpha_1]$.
The complex pair of nondimensional roots of the characteristic polynomial of (16) is

$$s = -\left(\frac{1}{4} + \chi_p\right)\hat{k}_p \pm j\left[\hat{k}_p^2\chi_p + \left(1 + \frac{1}{2}\hat{k}_s\chi_s\right)(1 + 2\hat{k}_s) - \left(\frac{1}{4} + \chi_p\right)^2\hat{k}_p^2\right]^{\frac{1}{2}} \tag{17}$$

where $\hat{k}_s = -k'_s/(h_w\omega_0) = -\hat{k}_{s1}/\hat{J}_{s1}$ and $\hat{k}_p = k'_p/\omega_0 = 4\hat{k}_s$. The damping coefficient ξ_p and the undamped precession frequency ω_p can be obtained as

$$\omega_p^2 = \hat{k}_p^2\chi_p + \left(1 + \frac{1}{2}\hat{k}_s\chi_s\right)(1 + 2\hat{k}_s)\ , \qquad \xi_p = \left(\frac{1}{4} + \chi_p\right)\frac{\hat{k}_p}{\omega_p}\ . \tag{18}$$

Clearly, the precession time constant is $((\frac{1}{4} + \chi_p)\hat{k}_p)^{-1}$ rad.

Nutation Control

Nutation amplitude as compared to precession amplitude is usually very small, hence we are primarily concerned with the angular rates rather than angular variations, which are mainly influenced by precession[2]. Furthermore, we must now consider the instantaneous roll/yaw components of the magnetic field instead of their orbit average values. These terms will be retained as constants, given the very small time constant associated with nutation. All the aforementioned considerations lead us to study the simplified system

$$\begin{aligned} I_1\ddot{\alpha}_1 + k_n\, b_3^2\,\dot{\alpha}_1 - (h_w + k_n\, b_1 b_3)\,\dot{\alpha}_3 = 0 \\ I_3\ddot{\alpha}_3 + k_n\, b_1^2\,\dot{\alpha}_3 + (h_w - k_n\, b_1 b_3)\,\dot{\alpha}_1 = 0 \end{aligned} \tag{19}$$

whose eigenvalues $s_{1,2} = -\xi_n\omega_n \pm j\omega_n\sqrt{1-\xi_n^2}$ have nutation damping and frequency given by

$$\begin{aligned} \xi_n &= \frac{k_n}{2\sqrt{I_1 I_3}}\frac{(B_1^2 I_1 + B_3^2 I_3)}{|h_w|} \\ \omega_n &= \frac{|h_w|}{\sqrt{I_1 I_3}}\ . \end{aligned}$$

In [2], a generalized nutation "time constant" was designated as $t_n = 2I_1I_3/[k_n(b_1^2I_1 + b_3^2I_3)]$ rad. t_n varies along the orbit, but cannot become neither negative nor infinity, implying that ξ_n will never be zero or negative, the indicators of instability. Then, the nutation gain can be designed such that a desired value is assigned to the average time constant $t_n = 2I_1I_3/[k'_n(\frac{1}{2}I_1 + 2I_3)]$.

Stability Analysis

The pole placement technique described in the previous Section makes several assumptions, that can be verified only a posteriori, *e.g.*, via Floquet theory. Fig. 3 portrays the closed loop characteristic multipliers relevant to the momentum bias satellite design case described in for the Lebsock-Eterno's law. The design parameters $\hat{k}_n$ and $\hat{k}_p$ were assigned values within the ranges $[0.01,\ 100]$ and $[0.75,\ 2.25]$ respectively, thus covering stable and unstable closed-loop systems as well. In the Figure, the closed loop system characteristic multipliers obtained by Floquet analysis are denoted by circles, whereas the results pertaining to the pole placement based method just discussed are marked by crosses.

Considering all the aforementioned restrictions and simplifications required by the pole placement based control synthesis procedure, the results are surprisingly good, matching impressively with those derived via Floquet theory. Notice that the slight deviations evidenced by the 5000x zoom in Fig. 3(d) are not relevant, since they are well inside the stability region marked by the red unit circle depicted in Fig. 3(c).

OPTIMAL PERIODIC DESIGN OF FIXED-GAIN PROJECTION-BASED CONTROLLERS

In this paper, we propose to compare pole placement methods with the approach to the tuning of projection-based controllers based on optimal periodic output feedback control problems [9, 4]. This approach relies on a gradient-based optimization method to determine time-periodic output feedback controllers by minimising a suitable quadratic cost function. In this Section, a short overview of this technique will be presented.

Consider the linear time-periodic system

$$x(k+1) = A(k)x(k) + B(k)u(k) \tag{20}$$

$$y(k) = C(k)x(k). \tag{21}$$

[2]It is here indirectly assumed that the precession part of $\alpha_1,\ \alpha_3$ is approximately constant during nutation.

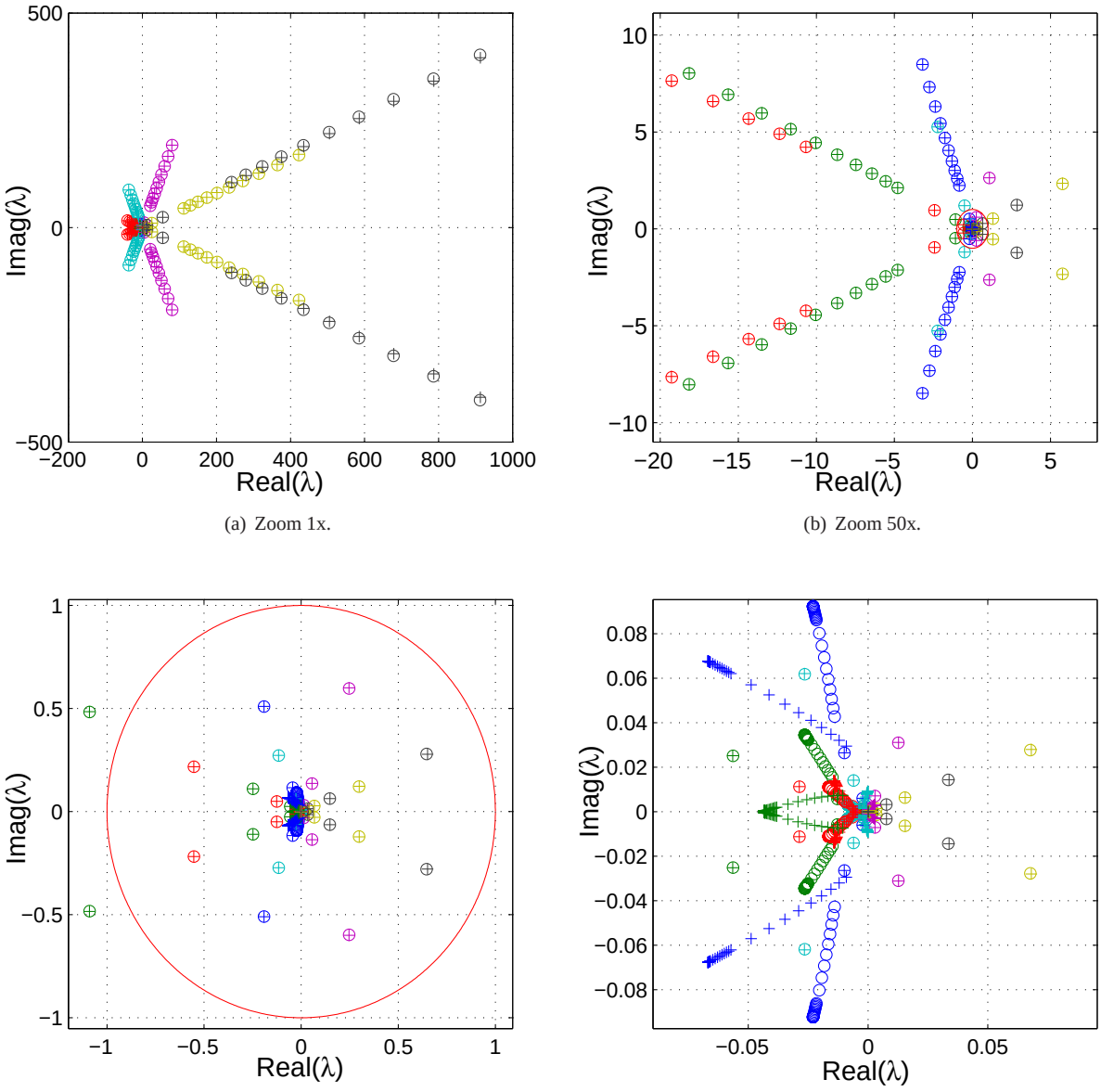

(a) Zoom 1x.

(b) Zoom 50x.

(c) Zoom 500x.

(d) Zoom 5000x.

Fig. 3. Comparison of closed-loop characteristic multipliers: Floquet theory (o) vs Pole placement (+). In the special case of a momentum bias spacecraft, the approximate stability results obtained via the pole placement-based design technique proposed in [2] match very accurately with the exact ones derived in the framework of Floquet theory.

The design problem entails minimizing the LQ criterion

$$J = E\left\{\sum_{k=0}^{\infty}\left[x(k)^T Q(k)x(k) + u(k)^T R(k)u(k)\right]\right\}, \tag{22}$$

where $Q(k) \geq 0$, $R(k) > 0$ are symmetric N-periodic matrices, in order to determine the optimal stabilizing constant gain output feedback controller, of the form

$$u(k) = Fy(k) = FC(k)x(k). \tag{23}$$

It is important to point out that the expected value in the definition of the criterion (22) is taken over the set of intial states and has nothing to do with time averagin as introduced in other approaches (see [2, 10]): the LQ optimisation problem is solved with respect to the time-periodic model (20)-(21). More precisely, it will be assumed in the following that the initial state x_0 is a random variable with zero mean and covariance $X_0 = E\left[x_0 x_0^T\right]$.

The proposed approach for the solution of this time-periodic design problem is based on the application of gradient-based optimisation techniques which exploit the possibility of efficiently computing both the cost function (22) and its gradient with respect to the parameters of the considered controller (23). The expressions of function and gradient can be computed on the basis of the following result (see [9] for details).

Proposition 1 *Let F be a constant stabilizing output feedback matrix and denote $\bar{A}(k) = A(k) + B(k)FC(k)$ and $\bar{Q}(k) = Q(k) + C^T(k)F^T R(k)FC(k)$. Then the expressions for the cost function* (22) *and its gradient with respect to the elements of F are given by*

$$J(F) = tr(P_0 X_0) \tag{24}$$

and

$$\nabla_F J(F) = 2\sum_{j=0}^{N-1}(R(j)FC(j) + B^T(j)P(j+1)\bar{A}(j))S(j)C^T(j) \tag{25}$$

where $P(k)$ and $S(k)$ satisfy, respectively, the discrete periodic Lyapunov equations (DPLEs)

$$P(k) = \bar{A}^T(k)P(k+1)\bar{A}(k) + Q(k), \quad P(N) = P(0) \tag{26}$$

and

$$S(k+1) = \bar{A}(k)S(k)\bar{A}^T(k) + G(k), \quad S(N) = S(0), \tag{27}$$

with

$$G(k) = \begin{cases} 0, & k \neq N-1 \\ X_0, & k = N-1. \end{cases}$$

From a numerical point of view, each evaluation of the performance index (22) and its gradient involves (see Proposition 1) the solution of a pair of DPLEs: a reverse time DPLE and a dual forward time DPLE, where it is assumed that all characteristic multipliers of the monodromy matrix of the closed loop system lie inside the open unit circle of the complex plane. This ensures existence of a unique solution of both equations. Note that for standard systems these are two discrete Lyapunov equations, which can be solved efficiently with a computational cost marginally greater than the cost of solving a single Lyapunov equation. The preservation of this feature is even more desirable for the periodic case, because of the much higher computational effort involved in solving a single periodic Lyapunov equation. Fortunately, this goal can be achieved with the recently proposed numerically stable algorithms to solve DPLEs [11]. The optimal tuning of the proposed control law (23) can be determined using a suitable function available in the Periodic Systems Toolbox [12]. This function is based on a gradient-based function minimization technique for problems with simple bounds (limited memory BFGS). To achieve the highest efficiency, the function and gradient evaluations have been implemented as a Fortran 95 *mex*-function based on the above results.

Remark 1 *Recently, the feasibility of techniques based on Linear and Bilinear Matrix Inequalities (LMI, BMI) for the design of periodic controllers has been explored [13]. While this approach lends itself to the formulation of more general control problems, it suffers from a significant drawback,* i.e., *it is limited to relatively small scale problems (both in terms of order and period) when compared to techniques relying on the solution of periodic Lyapunov and Riccati equations.*

In the framework of the present study, the above described approach has been applied to a discretised version of the LTP model defined by equations (11) and (13), together with the dynamic model for roll/yaw dynamics given by (4)-(5).

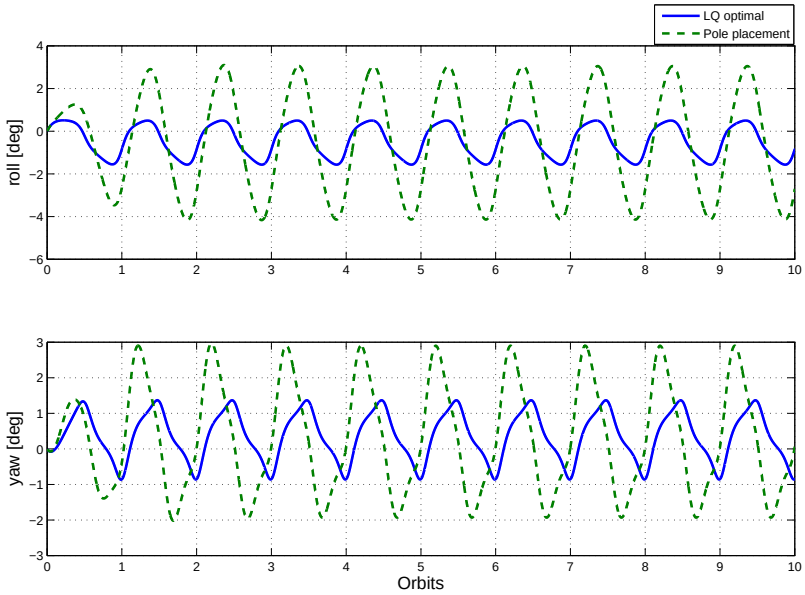

Fig. 4. Simulation of roll/yaw angles for a momentum bias satellite: Pole placement design (dashed lines) and LQ optimal design (solid lines).

SIMULATION RESULTS

The pole placement technique and the numerical optimized projection-based design were compared in a simulation study. Simulations refer to a momentum bias satellite on a circular orbit with 108° inclination. The resulting orbital period amounts to 9124.6 seconds, with an orbital angular rate of $0.00068860\ rad/s$. The momentum wheel angular momentum h_s was set to $-81.3491\ Kg \cdot m^2/s$, whereas the adopted satellite moments of inertia were $I_1 = 81.7789$, $I_2 = 76.0885$ and $I_3 = 60.2566\ Kg \cdot m^2$. All simulation data are taken from reference [2].

For the pole placement method the design parameters $\hat{k}_n$ and $\hat{k}_p$ were set to $\hat{k}_n = 10$ and $\hat{k}_p = 0.75$ respectively, which resulted in the best compromise possible between pointing accuracy and control effort. The obtained closed loop stability degree, computed a posteriori using Floquet theory, amounted to 0.284. The projection-based, numerically optimized output feedback design technique discussed in the previous Section was also used, in order to derive a stabilizing control law for the coupled roll/yaw dynamics. The search for a stabilizing controller was started with the solution adopted for the aforementioned pole placement design. Also, a full state feedback was considered, *i.e.*, the candidate K matrix in (8) was full. The achieved closed loop stability degree for the considered design was 0.128, which is a significant improvement over the preceding pole placement result.

Simulation results pertaining to the considered design methods are reported in Fig.s 4-6, where the behaviour of the closed-loop system in response to external disturbance torques due to a magnetic residual dipole is illustrated.

The relative roll/yaw angles are shown in Fig. 4. Notice that the relative angles are confined well within the ± 4 degrees interval, *i.e.*, within the linear region. The relative angular rates are shown in Fig. 5, while the applied pitch electromagnet dipole is depicted in Fig. 6. Also, notice that the required magnetic dipole is very small. The results evidence a significant improvement in performance over the pole placement based design. Also, this result is obtained by decreasing the required control action by more than 10%.

CONCLUDING REMARKS

The problem of designing a control law for magnetic control of the coupled roll/yaw dynamics of a momentum bias spacecraft has been considered. A pole placement approach based on an approximate time-invariant model and an optimisation approach based on the exact time-periodic model have been discussed and compared. Simulation results demonstrate that the optimisation approach can lead to a better design both in terms of stability degree and of steady state closed loop performance in response to cyclic disturbance torques.

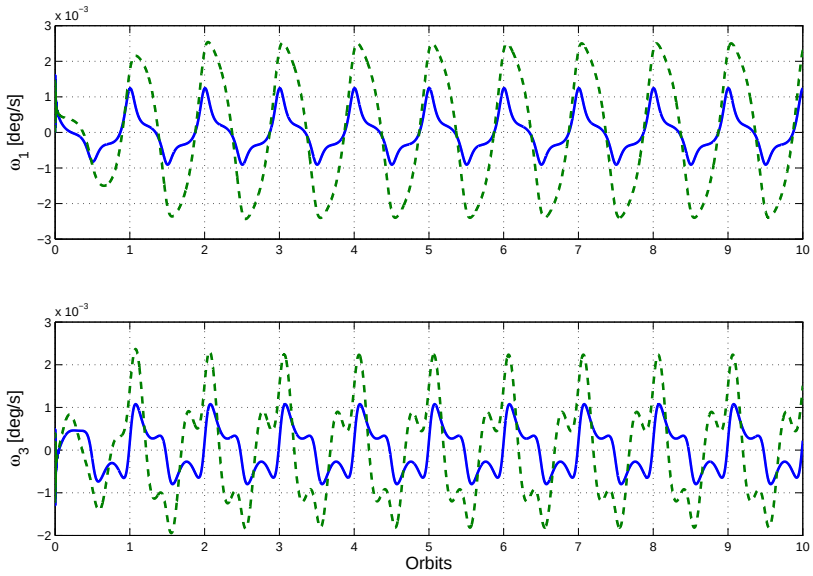

Fig. 5. Simulation of roll/yaw angular rates for a momentum bias satellite: Pole placement design (dashed lines) and LQ optimal design (solid lines).

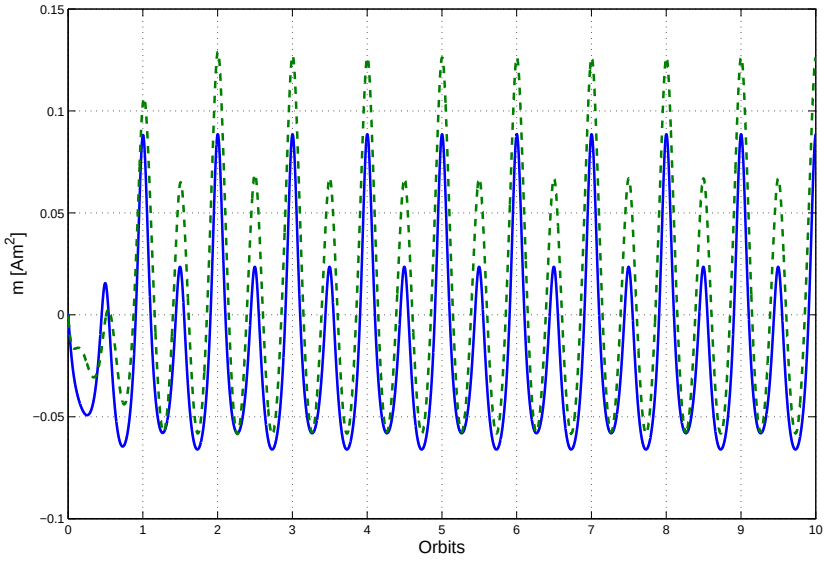

Fig. 6. Simulation of pitch magnetic dipole moment for a momentum bias satellite: Pole placement design (dashed lines) and LQ optimal design (solid lines).

REFERENCES

[1] A.C. Stickler and K.T. Alfriend. An elementary magnetic attitude control system. *Journal of Spacecraft and Rockets*, 13(5):282–287, 1976.

[2] H. B. Hablani. Comparative Stability Analysis and Performance of Magnetic Controllers for Bias Momentum Satellites. *Journal of Guidance, Control, and Dynamics*, 18(6):1313–1320, 1995.

[3] M. Psiaki. Magnetic torquer attitude control via asymptotic periodic linear quadratic regulation. *Journal of Guidance, Control and Dynamics*, 24(2):386–394, 2001.

[4] T. Pulecchi, M. Lovera, and A. Varga. Optimal discrete-time design of magnetic attitude control laws. In *Proceedings of the 6th International ESA Conference on Guidance, Navigation and Control Systems, Loutraki, Greece*, 2005.

[5] E. Silani and M. Lovera. Magnetic spacecraft attitude control: A survey and some new results. *Control Engineering Practice*, 13(3):357–371, 2005.

[6] P. Hughes. *Spacecraft attitude dynamics*. John Wiley and Sons, 1986.

[7] P. C. Wheeler. Spinning spacecraft attitude control via the environmental magnetic field. *Journal of Spacecraft and Rockets*, 4(12):1631–1637, 1967.

[8] K. Lebsock and J. Eterno. Design of a maneuverable momentum bias attitude control system. In *Proceedings of the AIAA/AAS Astrodynamics Conference, Minneapolis (MN), USA*, pages 704–713, 1988.

[9] A. Varga and S. Pieters. Gradient-based approach to solve optimal periodic output feedback control problems. *Automatica*, 34:477–481, 1998.

[10] H. B. Hablani. Pole-Placement Technique for Magnetic Momentum Removal of Earth-Pointing Spacecraft. *Journal of Guidance, Control, and Dynamics*, 20(12):268–275, 1997.

[11] A. Varga. Periodic lyapunov equations: some applications and new algorithms. *International Journal of Control*, 67(1):69–87, 1997.

[12] A. Varga. A periodic systems toolbox for Matlab. In *16th IFAC World Congress, Prague, Czech Republic*, 2005.

[13] C. Farges, D. Peaucelle, and D. Arzelier. Lmi formulation for the resilient dynamic output feedback stabilization of linear periodic systems. In *13th IFAC Workshop on Control Applications of Optimisation, Paris, France*, 2006.